

IOWA STATE UNIVERSITY

Digital Repository

Retrospective Theses and Dissertations

Iowa State University Capstones, Theses and
Dissertations

1-1-1960

Dimensional analysis of homogeneous nuclear reactor cores

Larry Lee Myers
Iowa State University

Follow this and additional works at: <https://lib.dr.iastate.edu/rtd>

Recommended Citation

Myers, Larry Lee, "Dimensional analysis of homogeneous nuclear reactor cores" (1960). *Retrospective Theses and Dissertations*. 18831.
<https://lib.dr.iastate.edu/rtd/18831>

This Thesis is brought to you for free and open access by the Iowa State University Capstones, Theses and Dissertations at Iowa State University Digital Repository. It has been accepted for inclusion in Retrospective Theses and Dissertations by an authorized administrator of Iowa State University Digital Repository. For more information, please contact digirep@iastate.edu.

**DIMENSIONAL ANALYSIS OF HOMOGENEOUS
NUCLEAR REACTOR CORES**

by

Larry Lee Myers

**A Thesis Submitted to the
Graduate Faculty in Partial Fulfillment of
The Requirements for the Degree of
MASTER OF SCIENCE**

Major Subject: Nuclear Engineering

Approved:

Signatures have been redacted for privacy

**Iowa State University
Of Science and Technology
Ames, Iowa**

1960

TABLE OF CONTENTS

	Page
I. INTRODUCTION	1
II. REVIEW OF LITERATURE	3
III. REACTOR DESIGN PARAMETERS	4
A. Development of Design Expression	4
B. Discussion of Parameters	9
IV. DIMENSIONAL ANALYSIS CONSIDERATIONS	23
A. Review of Dimensional Analysis	23
B. Application to Design Expression	24
C. Discussion of Pi Terms	26
V. INVESTIGATION OF OPERATIONAL REACTORS	30
A. LOPO	30
B. HYPO	30
C. RRR	31
D. SUPO	31
E. NAA-WBNS	32
VI. DESIGN CURVES	35
VII. SUMMARY AND CONCLUSIONS	46
VIII. SUGGESTIONS FOR FUTURE INVESTIGATIONS	48
IX. LITERATURE CITED	50
X. ACKNOWLEDGEMENTS	52

LIST OF FIGURES

	Page
Figure 1. τ vs. f_a^H	38
Figure 2. π_1 vs. π_4	39
Figure 3. π_1 vs. π_5	40
Figure 4. π_1 vs. π_6	41
Figure 5. π_1 vs. π_7	42
Figure 6. $\frac{1}{\pi_1}$ vs. π_8	43
Figure 7. π_1 vs. π_9	44
Figure 8. π_5 vs. π_9	45

LIST OF TABLES

	Page
Table 1. Geometric buckling for various reactor shapes	10
Table 2. Average number of neutrons per fission	12
Table 3. Dimensions of basic design parameters	25
Table 4. Proposed ρ terms	26
Table 5. Summary of operating reactor data and calculations	33

I. INTRODUCTION

The design of nuclear reactors is accomplished through long and tedious calculations, many of which presuppose the use of electronic computers. These methods permit a great degree of precision and can accurately predict the nuclear properties of the reactor under consideration. For many preliminary studies, however, the precision of the computer methods is not necessary. It may only be desired to give a rough estimate of the size or amount of fuel required to produce criticality in a proposed reactor. Through the calculations used for these rough approximations, various fuel-moderator combinations can be evaluated as well as the effects produced by varying enrichment, reactor shape, and component concentrations.

The purpose of this investigation is to attempt to relate the various reactor design parameters through dimensional analysis in order to obtain design curves which indicate the interdependence of the design parameters. These design curves are developed from data which has been obtained from operational reactors. By using operational reactor data, the variation between the actual values of the parameters and those values calculated theoretically is reduced and by using dimensionless groups in plotting the curves, the reactors lose their identification and appear as a reactor type independent of the individual reactors.

This investigation is limited to those reactors having the fuel and moderator combined in a homogeneous solution. The possibility of applying the dimensional analysis approach to heterogeneous reactors will be considered briefly. It should also be noted that this investigation is based on a just-critical reactor although it is felt that the application of the method to power producing reactors is possible.

II. REVIEW OF LITERATURE

A review of the literature pertaining to nuclear reactors and their design did not disclose a previous attempt to apply dimensional analysis techniques to the generation of design curves. In a letter to the editor [1, p. 269], S. Pearlstein proposed the possibility of applying similitude to nuclear engineering by using dimensionless groups to produce reactor models. Mr. Pearlstein suggested several possible dimensionless groups which could be used; however, he did not elaborate on their use. In his masters thesis [2], John C. MacAlpine III uses dimensional analysis to develop a method of designing reactor models which will retain the operational characteristics of the actual reactor. Mr. MacAlpine indicates the distortion of variables required to design the models and includes an example reactor problem which utilizes his method.

The sources of information used in this investigation are referred to throughout the paper and are indicated by enclosing the reference number in brackets.

III. REACTOR DESIGN PARAMETERS

The various methods of calculating the nuclear properties of reactors in order to determine the combination of components which will produce criticality depend upon a series of variables which are functions of the various chemical elements which comprise the fuel-moderator mixture. By using volume fraction weighting techniques, these individual variables for the component elements can be combined to produce a variable which is valid for the specific mixture under consideration. The parameters for the specific reactor are then formed from the volume-weighted variables by using the relationships which represent a just-critical reactor.

A. Development of Design Expression

The neutron economy in a reactor of infinite extent is represented by the four-factor formula which defines k_{∞} , the infinite multiplication factor [3, p. 84]

$$k_{\infty} = \eta \epsilon p f \quad (1)$$

where k_{∞} = number of neutrons of thermal energy produced by the reactor per thermal neutron absorbed.

η = average number of fast fission neutrons emitted per thermal neutron captured in fuel.

ϵ = fast fission factor = ratio of total number of neutrons produced by all fissions to number resulting from thermal neutron fissions.

p = resonance escape probability = fraction of fission neutrons escaping capture while being slowed down.

f = thermal utilization = fraction of thermal neutrons absorbed in fuel.

For a reactor of finite size, an effective multiplication factor, k_{eff} , is defined by accounting for the probability of leakage which is inherent with size reduction. In a critical reactor, it is necessary that this effective multiplication factor be no less than unity in order to provide a self-sustaining nuclear reaction. The leakage of neutrons from a finite reactor reduces the number of neutrons available, so it is common to define nonleakage probability terms to be applied to the infinite multiplication factor in order to obtain the effective multiplication factor [4, p. 107]

$$k_{\text{eff}} = k_{\infty} \mathcal{L}_f \mathcal{L}_t \quad (2)$$

where \mathcal{L}_f = fast leakage factor

\mathcal{L}_t = thermal leakage factor

The probability that the neutrons do not leak from the reactor between the time they are produced and the time they become thermalized is represented by [5, p. 174]

$$\mathcal{L}_f = e^{-B^2 \tau} \quad (3)$$

where B^2 = buckling

τ = age of thermal neutrons

The probability that the neutrons do not leak from the reactor between the time they are thermalized and the time they are

absorbed is represented by [5, p. 175]

$$\alpha_t = \frac{1}{1 + L^2 B^2} \quad (4)$$

where L = thermal diffusion length.

By combining Equations (2), (3), and (4), the critical equation is obtained [5, p. 176]

$$k_{\text{eff}} = 1 = \frac{k_{\infty} e^{-B^2 \tau}}{1 + L^2 B^2} \quad (5)$$

This equation is identical with the critical equation obtained by age-diffusion considerations in which the Fermi age treatment is applied to the neutrons during slowing down and diffusion theory is applied to the thermal neutrons.

By applying the relationships defining the variables, Equation (5) can be expressed in terms of the ten basic design variables which are used in this investigation. The product ηf can be represented by [5, pp. 178-179]

$$\eta f = \left(\nu \frac{\Sigma_f}{\Sigma_{\text{fuel}}} \right) \left(\frac{\Sigma_{\text{fuel}}}{\Sigma_a} \right) = \nu \frac{\Sigma_f}{\Sigma_a} \quad (6)$$

where ν = average number of fast neutrons per fission.

Σ_f = macroscopic cross section for fission by thermal neutrons.

Σ_{fuel} = total macroscopic cross section for absorption of thermal neutrons in fuel by both fission and nonfission processes.

Σ_a = total macroscopic cross section for absorption of thermal neutrons in all reactor core material.

The resonance escape probability, p , can be expressed as a function of energy by [3, p. 253]

$$p(E) = \exp \left[- \frac{N_0}{\bar{\xi} \Sigma_s} \int_E^{E_0} \left(\sigma_{ao} \frac{\Sigma_s}{\Sigma_s + \Sigma_a} \right) \frac{dE'}{E'} \right] \quad (7)$$

where N_0 = atoms of resonance absorber per unit volume

$\bar{\xi}$ = average of the logarithmic energy decrement per collision

Σ_s = total macroscopic scattering cross section

E_0 = fission neutron energy

E = thermal neutron energy

σ_{ao} = absorption cross section for neutrons of energy E'

The integral in Equation (7) is defined as the effective resonance integral, RI , and has been shown empirically to be represented by [3, p. 256] and [6, p. 43]

$$RI = \int_E^{E_0} \left(\sigma_{ao} \frac{\Sigma_s}{\Sigma_s + \Sigma_a} \right) \frac{dE'}{E'} = C_1 \left(\frac{\Sigma_s}{N_0} \right)^{C_2} \quad (8)$$

where C_1 and C_2 are empirically determined constants which are specific for a given resonance absorber. By combining Equations (7) and (8), the expression for p is given by

$$\begin{aligned} p &= \exp \left[- \frac{N_0}{\bar{\xi} \Sigma_s} C_1 \left(\frac{\Sigma_s}{N_0} \right)^{C_2} \right] \\ &= \exp \left[- \frac{C_1}{\bar{\xi}} \left(\frac{N_0}{\Sigma_s} \right)^{1-C_2} \right] \end{aligned} \quad (9)$$

By introducing the thermal microscopic cross section for the resonance absorber, σ_{aT} , the resonance escape probability can be expressed in terms of the thermal macroscopic cross section for the resonance absorber, Σ_{aR}^{th}

$$\begin{aligned}
 p &= \exp \left[- \frac{C_1}{\xi} \left(\frac{N_O}{\Sigma_S} \right)^{1-C_2} \left(\frac{\sigma_{aT}}{\sigma_{aT}} \right)^{1-C_2} \right] \\
 &= \exp \left[- \frac{C_1}{\xi \sigma_{aT}^{1-C_2}} \left(\frac{\Sigma_{aR}^{th}}{\Sigma_S} \right)^{1-C_2} \right] \\
 &= \exp \left[- \frac{C_3}{\xi} \left(\frac{\Sigma_{aR}^{th}}{\Sigma_S} \right)^{C_4} \right]
 \end{aligned} \tag{10}$$

where C_3 = a constant formed by combining C_1 with the value of σ_{aT} raised to the $1-C_2$ power

$$C_4 = 1-C_2$$

The square of the thermal diffusion length, L^2 , can be defined as [3, p. 116]

$$L^2 = \frac{D}{\Sigma_a} \tag{11}$$

where D = diffusion coefficient

By substituting Equations (1), (6), (10), and (11) into Equation (5), the critical condition can be expressed in terms of ten basic design parameters

$$k_{eff} = 1 = \frac{\epsilon v \frac{\Sigma_f}{\Sigma_a} \exp \left[- \frac{C_3}{\xi} \left(\frac{\Sigma_{aR}^{th}}{\Sigma_S} \right)^{C_4} \right] \exp [-B^2 \tau]}{1 + \frac{DB^2}{\Sigma_a}} \tag{12}$$

B. Discussion of Parameters

1. B^2 , buckling [3, p. 198]

By utilizing the diffusion equation [3, p. 101]

$$D\nabla^2\phi - \Sigma_a\phi + S = \frac{\partial n}{\partial t} \quad (13)$$

where D = diffusion coefficient

∇^2 = Laplacian operator

ϕ = thermal neutron flux

Σ_a = macroscopic absorption cross section

S = source term

$\frac{\partial n}{\partial t}$ = time rate of change of neutron density

in conjunction with Fermi age theory to define the source term, a wave equation is obtained of the form

$$\nabla^2\phi(r) + B^2\phi(r) = 0 \quad (14a)$$

where B^2 = buckling

$\phi(r)$ = neutron flux at a point r

Equation (14a) can be put in form

$$B^2 = - \frac{\nabla^2\phi(r)}{\phi(r)} \quad (14b)$$

where the buckling is seen to be a measure of the curvature of the neutron flux at a point r in the system. Two types of buckling can be defined. The material buckling, B_m^2 , is a property only of the composition of the multiplying medium and satisfies Equation (5) as well as Equation (14a). The geo-

metric buckling, B_g^2 , is a property only of the size and shape of the reactor. By solving Equation (14a) for various shapes, expressions for the geometric buckling can be obtained. Table 1 presents these expressions for several commonly used reactor shapes in terms of height H , radius R , and edge lengths a , b , and c . These dimensions all include the extrapolation distance, d , which is defined by [3, p. 104]

$$\begin{aligned} d &= 0.71 \lambda_t \\ &= \frac{0.71}{\Sigma_s (1 - \bar{\mu}_0)} \\ &\approx 0.71 (3D) \end{aligned} \quad (15)$$

where λ_t = transport mean free path

$\bar{\mu}_0$ = average cosine of the scattering angle per collision

Table 1. Geometric buckling for various reactor shapes

Shape	B_g^2
Sphere	$\left(\frac{\pi}{R}\right)^2$
Parallelepiped	$\left(\frac{\pi}{a}\right)^2 + \left(\frac{\pi}{b}\right)^2 + \left(\frac{\pi}{c}\right)^2$
Cube	$3\left(\frac{\pi}{H}\right)^2$
Cylinder	$\left(\frac{2.405}{R}\right)^2 + \left(\frac{\pi}{H}\right)^2$

It is shown that for a just-critical reactor, the material buckling is identically equal to the geometric buckling. In the remainder of this investigation, no distinction will be made between material and geometric buckling and the buckling

will be designated by B^2 .

2. ϵ , fast fission factor [5, p. 178]

The fast fission factor, ϵ , accounts for the fact that some fission occurs before the fission neutrons have reached thermal energy. This effect is due primarily to the fission of U^{238} and Th^{232} by neutrons having energies above 1 Mev. The other nuclear fuels, U^{235} , U^{233} and Pu^{239} , all have small fission cross sections in this energy region.

The value of the fast fission factor varies considerably with reactor type, fuel enrichment and fuel composition. For natural uranium with either graphite or heavy water as moderator, a value of 1.03 has been found [3, p. 83]. A maximum value of 1.19 has been found for natural uranium [7, p. 707]. The fast fission factor in a heterogeneous reactor varies with the size of the fuel rods. For homogeneous reactors the value of 1.00 is valid [5, p. 178]. Since this investigation is limited to the consideration of homogeneous reactors, the value of ϵ will be assumed to have a constant value of unity.

3. ν , fast neutrons per thermal neutron fission [5, p. 30]

The average number of neutrons released during each act of thermal fission is a constant for each nuclear fuel. These values are larger than the corresponding values of η , the

average number of neutrons released per thermal neutron absorbed in fissionable fuel, by the factor $\frac{\Sigma_{\text{fuel}}}{\Sigma_f}$ which

accounts for parasitic capture. Table 2 lists the values for ν as reported in [8] and [9].

Table 2. Average number of neutrons per fission

Fissionable fuel	ν
U^{233}	2.51
U^{235}	2.43
Pu^{239}	2.89

4. Σ_f , macroscopic fission cross section [3, p. 45]

In general, a macroscopic cross section, Σ , refers to the total cross section of the nuclei in a cubic centimeter of material while the microscopic cross section, σ , applies to a single nucleus. The relation between the two is given by

$$\Sigma = N\sigma \quad (16)$$

In this equation, N is the number of nuclei per cubic centimeter and is defined by

$$N = \frac{\rho N_0}{A} \quad (17)$$

where ρ = density of the material

N_0 = Avogadro's number

= 0.6023×10^{24} atoms (or nuclei) per gram atom

A = atomic weight of the material

For a compound containing 1 different nuclear species, the macroscopic cross section is given by

$$\begin{aligned}\Sigma &= N_1\sigma_1 + N_2\sigma_2 + \dots + N_1\sigma_1 \\ &= \frac{\rho N_O}{M} (v_1\sigma_1 + v_2\sigma_2 + \dots + v_1\sigma_1)\end{aligned}\quad (18)$$

where M = molecular weight of the compound

v = number of atoms per molecule

In the course of this investigation, it is more advantageous to use Equation (18) in a form involving weight fractions so that the cross section information for cooling coils and experimental tubes located within the core can be included. The form used is

$$\Sigma = \rho N_O \left(\frac{f_{w1}\sigma_1}{A_1} + \frac{f_{w2}\sigma_2}{A_2} + \dots + \frac{f_{w1}\sigma_1}{A_1} \right) \quad (19)$$

where ρ = "core density" including fuel-moderator solution and tubes

f_w = weight fraction of each species

Equation (19) is applicable to fission, scattering, absorption and total cross sections.

The macroscopic fission cross section varies with the fuel-to-moderator ratio and with the fuel enrichment as well as with the operating temperature. The values used in this investigation are calculated by Equation (19) using microscopic fission cross section values from [8], [9] and [10] after applying the temperature correction [11, p. 177]

$$\sigma_2 = \sigma_1 \sqrt{\frac{T_1}{T_2}} \quad (20)$$

where σ_2 = microscopic cross section at operating temperature

σ_1 = microscopic cross section recorded in tables

T_2 = absolute temperature of reactor

T_1 = absolute temperature at which cross sections are
compiled

5. Σ_a , macroscopic absorption cross section [4, p. 39]

The macroscopic absorption cross section varies with the composition of the core and with the operating temperature. The values for this investigation are calculated by using Equations (19) and (20) with microscopic data from [8], [9], [10], [12] and [13]. The largest contributions to the macroscopic absorption cross sections in this investigation are made by the U^{235} and the hydrogen, so that the fuel-to-moderator ratio and the fuel enrichment are of prime importance.

6. Σ_s , macroscopic scattering cross section [3, p. 50]

The macroscopic scattering cross section, Σ_s , varies with core composition and is calculated by using Equations (19) and (20) in conjunction with cross section data from [4], [8], [9], [12] and [13]. In this investigation the values of Σ_s are influenced primarily by hydrogen and oxygen.

7. Σ_{aR}^{th} , thermal macroscopic cross section for resonance absorber [7, p. 83]

The thermal macroscopic cross section for the resonance absorber as used in the expression for the resonance escape probability is dependent only upon the concentration of the resonance absorber. The expression used to calculate Σ_{aR}^{th} in this investigation is

$$\Sigma_{aR}^{th} = \frac{\rho N_O f_{wR} \sigma_{aT}}{A_R} \quad (21)$$

where ρ = "core density" including fuel-moderator solution and tubes

N_O = Avogadro's number

f_{wR} = weight fraction of resonance absorber

σ_{aT} = thermal absorption cross section for resonance absorber

A_R = atomic weight of resonance absorber

The two resonance absorbers of interest in reactor calculations are U^{238} and Th^{232} having σ_{aT} values of 2.75 and 7.0 barns, respectively [7, p. 83].

In this investigation, since all the reactors considered are fueled by uranium, the resonance absorption is due to U^{238} . At high enrichments (low concentrations of U^{238}) the values of Σ_{aR}^{th} become exceedingly small.

8. ξ , average logarithmic energy decrement [3, p. 143]

The average logarithmic energy decrement per collision, ξ , is defined as the average value of the change in the logarithm of the neutron energy for a single collision, i.e.,

$$\begin{aligned}\xi &= \overline{\ln E_1 - \ln E_2} \\ &= \ln \overline{\frac{E_1}{E_2}}\end{aligned}\quad (22)$$

where E_1 = energy of the neutron before collision

E_2 = energy of the neutron after collision

Since the energy loss per collision decreases as the mass of the target nuclei increases, the value of ξ is dependent upon the atomic weight of the medium. For elements having atomic weights larger than about ten, the value of ξ can be approximated by

$$\xi \approx \frac{2}{A + \frac{2}{3}} \quad (23)$$

Values for ξ range from 1.000 for hydrogen to 0.0077 for the heaviest nuclei. For a mixture or compound containing i different nuclei, the mean value of average logarithmic energy decrement, $\bar{\xi}$, is defined by [5, p. 157]

$$\begin{aligned}\bar{\xi} &= \frac{\Sigma_{s1}\xi_1 + \Sigma_{s2}\xi_2 + \dots + \Sigma_{si}\xi_i}{\Sigma_{s1} + \Sigma_{s2} + \dots + \Sigma_{si}} \\ &= \frac{\Sigma_{s1}\xi_1 + \Sigma_{s2}\xi_2 + \dots + \Sigma_{si}\xi_i}{\Sigma_s}\end{aligned}\quad (24)$$

where Σ_{s1} = macroscopic scattering cross sections for individual species

ξ_1 = average logarithmic energy decrement for the individual species

Σ_s = total scattering cross section for the core as previously discussed

For this investigation, Equation (24) is used in a form similar to that of Equation (19)

$$\bar{\xi} = \frac{\rho N_O}{\Sigma_s} \left(\frac{f_{w1} \sigma_{s1} \xi_1}{A_1} + \frac{f_{w2} \sigma_{s2} \xi_2}{A_2} + \dots + \frac{f_{wi} \sigma_{si} \xi_i}{A_i} \right) \quad (25)$$

where all variables are as previously defined. For the reactors considered in this investigation, hydrogen and oxygen make the largest contributions. The values for ξ_i are obtained from [12].

9. D, diffusion coefficient [3, p. 92]

The diffusion coefficient, D, arises from the application of Fick's law of diffusion which is the basic assumption of elementary diffusion theory. The expression for D is [3, p. 97]

$$D = \frac{1}{3\Sigma(1 - \bar{\mu}_0) \left(1 - \frac{4}{5} \cdot \frac{\Sigma_a}{\Sigma} + \frac{\Sigma_a}{\Sigma} \cdot \frac{\bar{\mu}_0}{1 - \bar{\mu}_0} + \dots \right)} \quad (26)$$

where Σ = total macroscopic cross section

$$= \Sigma_a + \Sigma_s$$

For materials having Σ_a much less than Σ_s , which is the case for the reactors considered in this investigation, Equation (26) reduces to [5, p. 135]

$$D = \frac{1}{3\Sigma_s(1 - \bar{\mu}_0)} \quad (27)$$

A convenient form of Equation (27) for use in this investigation is

$$\begin{aligned} \frac{1}{D} &= 3\Sigma_s(1 - \bar{\mu}_0) \\ &= 3\rho N_O \left[\frac{f_{w1}\sigma_{s1}(1-\mu_0)_1}{A_1} + \frac{f_{w2}\sigma_{s2}(1-\mu_0)_2}{A_2} \right. \\ &\quad \left. + \dots + \frac{f_{wi}\sigma_{si}(1-\bar{\mu}_0)_i}{A_i} \right] \end{aligned} \quad (28)$$

where all quantities are as previously defined and the values of σ_{s1} and $(1-\bar{\mu}_0)_1$ are obtained from [4], [8], [9] and [12]. In this investigation, the main influence on the value of D is exerted by hydrogen, oxygen and U^{235} .

10. τ , neutron age [11, p. 58]

The neutron age, τ , in a reactor is related to the energy of the neutron and is proportional to the average of the squares of all of the straight-line paths from the source to the point where a neutron reaches a certain energy. The value of interest in this investigation is the age-to-thermal,

i.e., the age corresponding to the decrease in neutron energy from fission energy (2 Mev) to thermal energy (0.025 ev). The neutron age has been determined experimentally for many substances of interest in reactor design. However, for the solutions contained in the cores of the reactors to be considered later in this investigation, tabulated age data were not available. Many exact methods for the theoretical determination of neutron age have been derived, several of which require special computer techniques.

The method to be used in this investigation is the semi-empirical Flügge-Tittle method for mixtures of heavy elements with hydrogen [11, p. 278]. This method determines the age-to-thermal by dividing the energy range into two sections. The upper section involves the portion of the energy range in which the scattering cross section of hydrogen varies largely with energy (2 Mev to approximately 100 kev) and it is assumed that the slowing down in this region is due to collisions with hydrogen. From the definition of the logarithmic energy decrement, Equation (22), which has a value of 1.0 for hydrogen, it is seen that

$$\begin{aligned}
 E_2 &= \frac{E_1}{\text{antilog } \xi} \\
 &= \frac{E_1}{\text{antilog } 1.0} \\
 &= \frac{E_1}{2.72}
 \end{aligned}
 \tag{29}$$

By applying Equation (29) three times, it is seen that after a third collision with hydrogen the energy of the neutron has been reduced to approximately 100 kev. It is shown that the mean square displacement for a collision is equal to $2\lambda^2$, where λ is the mean free path at the energy before collision. The total mean square displacement for the three collisions required to reduce the neutron energy to 100 kev is therefore given by

$$\overline{r^2}(2 \text{ Mev to } 100 \text{ kev}) = 2\lambda_1^2 + 2\lambda_2^2 + 2\lambda_3^2 \quad (30)$$

By definition, the slowing-down length is given by

$$\begin{aligned} l_s^2 &= \frac{\overline{r^2}}{6} \\ &= \frac{\lambda_1^2 + \lambda_2^2 + \lambda_3^2}{3} \end{aligned} \quad (31)$$

where l_s^2 = slowing down length from 2 Mev to 100 kev

The values for the mean free paths to be used in Equation (31) are obtained from the empirical equation [11, p. 279]

$$\lambda_1 = \lambda \left(2.155 - 0.119 \frac{\lambda_{\text{other}}}{\lambda_H} \right) \quad (32)$$

where λ_1 = neutron mean free path corresponding to energy E_1 to be used in Equation (31) where 1 takes the values 1, 2 and 3

λ = mean free path in mixture corresponding to an energy E_1
 $= \frac{1}{\Sigma_S}$

λ_{other} = mean free path in all material except hydrogen
corresponding to an energy E_i

$$= \frac{1}{(\Sigma_S)_{\text{other}}}$$

λ_H = mean free path in hydrogen corresponding to an
energy E_i

$$= \frac{1}{(\Sigma_S)_H}$$

The values for Σ are calculated as mentioned previously.

For the lower section of the energy range (100 kev to 0.025 ev) the Fermi age equation is valid and the age is given by [11, p. 279]

$$\tau(100 \text{ kev to } 0.025 \text{ ev}) = \int_{0.025 \text{ ev}}^{100 \text{ kev}} \frac{\frac{dE}{E}}{3\xi\Sigma_S(1-\mu_0)\Sigma_S} \quad (33)$$

where $\xi\Sigma_S = \rho N_O \left(\frac{f_{w1}\sigma_{s1}\xi_1}{A_1} + \frac{f_{w2}\sigma_{s2}\xi_2}{A_2} + \dots + \frac{f_{wj}\sigma_{sj}\xi_j}{A_j} \right)$

$$\frac{\xi\Sigma_S}{(1-\mu_0)\Sigma_S} = \rho N_O \left[\frac{f_{w1}\sigma_{s1}(1-\mu_0)_1}{A_1} + \frac{f_{w2}\sigma_{s2}(1-\mu_0)_2}{A_2} \right. \\ \left. + \dots + \frac{f_{wj}\sigma_{sj}(1-\mu_0)_j}{A_j} \right]$$

for a mixture containing j nuclear species.

The final age-to-thermal is then given by

$$\tau_{th} = l_s^2 + \tau(100 \text{ kev to } 0.025 \text{ ev}) \quad (34)$$

In this investigation, the numerical integration of Equation (33) for the various fuel solutions gave nearly a constant value, within the accuracy of the method, so that the form of Equation (34) actually used was

$$\tau_{th} = K l_s^2 \quad (35)$$

where K = constant determined by numerical integration.

It has been shown [2, p. 21] that the Flügge-Tittle method gives values which agree well with experiment for mixtures having an atom fraction of hydrogen larger than 0.45.

IV. DIMENSIONAL ANALYSIS CONSIDERATIONS

A brief review of dimensional analysis techniques will be given in this section followed by the application of dimensional analysis to the design expression developed in the previous section. A proposed list of nine pi terms will then be discussed.

A. Review of Dimensional Analysis [14]

Dimensional analysis is a tool which relates variables through their fundamental dimensions, rather than through the absolute numerical values of the variables, in order to eliminate differences in the methods of measurement. By applying dimensional analysis to physical phenomenon, dimensionless groups can be determined which are interrelated and can be used for predicting the outcome of changes in the magnitude of the dimensional variables comprising the dimensionless groups.

In general, a dependent variable, α , can be expressed in terms of a functional relationship involving the variables upon which it depends [14, p. 21]

$$\alpha = f(a_1, a_2, \dots, a_n) \quad (36)$$

where the various a 's are the n independent variables determining α . For many problems, the relationship between the dependent and independent variables is obtained easily by experimental methods. In cases where the experimental deter-

mination of the relationships is inconvenient or time-consuming, the Buckingham Pi Theorem provides a means of reducing the number of variables by grouping the variables into dimensionless groups designated as pi terms. The Buckingham Pi Theorem states that the number of independent pi terms required, s , is equal to the number of variables concerned minus the number of fundamental dimensions required to express the variables [14, p. 36]. A functional relationship between the pi terms can then be expressed as

$$\pi_1 = F(\pi_2, \pi_3, \dots, \pi_s) \quad (37)$$

It may then be possible to determine experimentally the interrelation among the pi terms.

B. Application to Design Expression

Following the techniques of dimensional analysis, the design expression given by Equation (12) can be written in functional notation as

$$B^2 = f(\epsilon, v, \Sigma_f, \Sigma_a, \Sigma_s, \Sigma_{aR}^{th}, \bar{\xi}, D, \tau) \quad (38)$$

where B^2 is arbitrarily chosen as the dependent variable.

This choice proves to be useful, since the critical size of a reactor is frequently desired and can be obtained easily from the buckling. A tabulation of the ten design parameters together with their dimensions is presented in Table 3.

It is apparent from Table 3 that only one dimension is involved so that application of the Buckingham Pi Theorem

Table 3. Dimensions of basic design parameters

Parameter	Dimension
B^2 , buckling	Length ⁻²
ϵ , fast fission factor	--
ν , fast neutrons per thermal neutron fission	--
Σ_f , macroscopic fission cross section	Length ⁻¹
Σ_a , macroscopic absorption cross section	Length ⁻¹
Σ_s , macroscopic scattering cross section	Length ⁻¹
Σ_{aR}^{th} , thermal macroscopic cross section for resonance absorber	Length ⁻¹
$\bar{\xi}$, average logarithmic energy decrement	--
D , diffusion coefficient	Length
τ , neutron age	Length ²

indicates nine independent pi terms are required to express the relationship. By inspection of Equation (12) in conjunction with Table 3, the proposed list of independent pi terms presented in Table 4 is developed. By using the pi terms listed in Table 4, the functional relationship between the dimensionless groups depicting a critical reactor is given by

$$\frac{B^2 D}{\Sigma_{aR}^{th}} = F(\epsilon, \nu, \bar{\xi}, \Sigma_f^2 \tau, \frac{\Sigma_f}{\Sigma_a}, \frac{\Sigma_{aR}^{th}}{\Sigma_a}, \frac{\Sigma_{aR}^{th}}{\Sigma_s}, \frac{D}{\tau \Sigma_a}) \quad (39)$$

Table 4. Proposed pi terms

π_1	$\frac{B^2 D}{\Sigma_{aR}^{th}}$
π_2	ϵ
π_3	v
π_4	$\bar{\xi}$
π_5	$\Sigma_f^{2\tau}$
π_6	$\frac{\Sigma_f}{\Sigma_a}$
π_7	$\frac{\Sigma_{aR}^{th}}{\Sigma_a}$
π_8	$\frac{\Sigma_{aR}^{th}}{\Sigma_s}$
π_9	$\frac{D}{\tau \Sigma_a}$

C. Discussion of Pi Terms

$$1. \pi_1 = \frac{B^2 D}{\Sigma_{aR}^{th}}$$

The value of $\frac{B^2 D}{\Sigma_{aR}^{th}}$ is dependent primarily on the value of Σ_{aR}^{th} , since the values of B^2 and D are relatively constant for a solution type. As previously discussed, Σ_{aR}^{th} is enrichment dependent so that it would be expected that the value of

$\frac{B^2D}{\Sigma_{aR}^{th}}$

would be quite small for reactors having low enrichment and increasingly larger for higher enrichments, having the theoretical limits of zero and infinity.

2. $\pi_2 = \epsilon$

As mentioned previously, the value of ϵ for homogeneous reactors is assumed to have a constant value of unity. For the various designs of heterogeneous reactors this π_1 term could take variable values depending upon reactor type, fuel and enrichment.

3. $\pi_3 = \nu$

Since the value of ν is dependent only upon the fissionable isotope utilized as fuel, it will have a constant value in this investigation.

4. $\pi_4 = \bar{\xi}$

As noted, the average logarithmic energy decrement is essentially a scattering or slowing-down property of a system and would therefore be expected to vary with the fraction of scattering nuclei (hydrogen) present. The variation of $\bar{\xi}$ would not be expected to be large in this investigation, however, since the fuel solutions are all water solutions of a uranyl compound precluding the same general composition requirements within the upper limit of solubility and the lower

limit of a dilution making criticality impossible.

$$5. \quad \pi_5 = \Sigma_f^2 \tau$$

The value of Σ_f depends upon the atom fraction of fissionable isotope present and, therefore, on the critical mass which varies with enrichment, core configuration and component concentrations. The value of τ is essentially a slowing-down property and is therefore dependent on the atom fraction of hydrogen present. For this investigation, it would be expected that the value of Σ_f would exhibit a larger relative variation than τ since the enrichment in a homogeneous aqueous system has wider limits than the hydrogen concentration. In view of this, the value of $\Sigma_f^2 \tau$ is expected to vary with the critical mass.

$$6. \quad \pi_6 = \frac{\Sigma_f}{\Sigma_a}$$

Both Σ_f and Σ_a are primarily dependent upon the amount of fissionable isotope present, so that the value of $\frac{\Sigma_f}{\Sigma_a}$ would be expected to be approximately constant with small variations to account for absorption by hydrogen.

$$7. \quad \pi_7 = \frac{\Sigma_{aR}^{th}}{\Sigma_a}$$

The previously mentioned dependence of Σ_{aR}^{th} on enrichment is much larger than the dependence which Σ_a has on U^{235} concentration, so that the value of $\frac{\Sigma_{aR}^{th}}{\Sigma_a}$ would be expected to

depend primarily on Σ_{aR}^{th} . This would indicate large values for low enrichment and small values for high enrichment.

$$8. \quad \pi_8 = \frac{\Sigma_{aR}^{th}}{\Sigma_S}$$

The value of Σ_S is dependent mainly upon the scattering nuclei concentration, so that small variation is expected for the reactors studied in this investigation. Therefore, the value of $\frac{\Sigma_{aR}^{th}}{\Sigma_S}$ would be expected to vary with Σ_{aR}^{th} in the same way described for $\frac{\Sigma_{aR}^{th}}{\Sigma_a}$.

$$9. \quad \pi_9 = \frac{D}{\tau \Sigma_a}$$

Both D and τ are properties of the scattering nuclei in the system and would tend to cancel each other's effect on $\frac{D}{\tau \Sigma_a}$. The value of π_9 would therefore be primarily dependent upon Σ_a and would vary inversely with the critical mass.

V. INVESTIGATION OF OPERATIONAL REACTORS

As examples of operational homogeneous reactors to be used in this investigation, five reactors of the water boiler type have been considered. Although it is realized that definite results cannot be expected from only five points, the reactors chosen were the only ones of the homogeneous type for which sufficient data to prepare complete calculations were readily available. The following sections briefly describe the five reactors and Table 5 summarizes the results of the calculations made.

A. LOPO

The zero-power reactor designated as LOPO (low power) was located at Los Alamos and became critical in May 1944. The core consisted of a 1/32-inch thick stainless steel sphere 1 foot in diameter containing uranyl sulfate in 13 liters of water. The critical mass was found to be 565 grams of U^{235} contained in uranium having an enrichment of 14.5%. The solution had a density of 1.348 g/cm.³ at the operating temperature of 39° C. The core was surrounded by a beryllium oxide reflector. The references containing information pertinent to LOPO are [5], [6], [15], [16], and [17].

B. HYPO

In December 1944, the reactor designated HYPO (high power) became critical at Los Alamos to replace LOPO. This

reactor was designed for operation at 1 kw and contained cooling water coils and an experimental tube. The core was a 1/16-inch thick stainless steel sphere 1 foot in diameter and containing 13.65 liters of uranyl nitrate solution. The uranium enrichment for this reactor was 14.0% and a critical mass of 808 grams of U^{235} was required. The reactor operated at 85° C. and had a solution density of 1.615 g/cm.³ A beryllium oxide reflector surrounded the core. The references pertaining to HYPO are [5], [6], [15], [16] and [17].

C. RRR

The reactor designated RRR (Raleigh Research Reactor) was built at North Carolina State College and designed for a power output of 10 kw. The reactor attained criticality in September 1953. The core was in the form of a 1/16-inch thick stainless steel cylinder having an inner diameter of 10 3/4 inches and a height of 11 inches. Included in the core were stainless steel cooling coils and experimental tubes. The critical mass of 787 grams of U^{235} was contained in 12.565 liters of uranyl sulfate solution having a density of 1.10 g/cm.³ and a maximum temperature of 80° C. The uranium enrichment was 90%. The core was enclosed by a graphite reflector. Information concerning RRR was found in [4], [5], [15] and [17].

D. SUPO

In February 1950, modifications were completed which changed the Los Alamos water boiler reactor to the 45 kw

reactor designated as SUPO (super power). The core structure was a stainless steel sphere having a 1 foot diameter and included cooling coils and experimental tubes. The 777-gram U^{235} critical mass was contained in 12.7 liters of uranyl nitrate solution having a density of 1.1 g/cm.³ The uranium enrichment was 88.7%. A graphite reflector surrounded the reactor. The information relating to SUPO was found in [5], [15] and [17].

E. NAA-WBNS

The reactor designated as NAA-WBNS (North American Aviation Water Boiler Neutron Source) attained criticality in April 1952. The core was in the form of a 1/16-inch thick stainless steel sphere having a diameter of 1 foot and equipped with an experimental tube. The solution used was uranyl nitrate containing a critical mass of 633.9 grams of U^{235} and having a density of 1.1 g/cm.³ The uranium was enriched to 90% in U^{235} . The core was surrounded by a graphite reflector. The information concerning NAA-WBNS was found in [15], [18] and [19].

Table 5. Summary of operating reactor data and calculations

	LOPO	HYP0	RRR	SUPO	NAA-WBNS
Shape	sphere	sphere	cylinder	sphere	sphere
Solution	UO ₂ SO ₄	UO ₂ (NO ₃) ₂	UO ₂ SO ₄	UO ₂ (NO ₃) ₂	UO ₂ (NO ₃) ₂
Enrichment, %U ²³⁵	14.5	14.0	90	88.7	90
Critical mass U ²³⁵ , g.	565	808	787	777	634
Temperature, °C.	39	85	80	85	39
f _a ^H , atom fraction H, %	63.25	58.40	64.95	63.60	65.40
B ² , cm. ⁻²	0.0389	0.0388	0.0396	0.0388	0.0392
Σ _f , cm. ⁻¹	0.0545	0.0772	0.0816	0.0765	0.0740
Σ _a , cm. ⁻¹	0.0860	0.1175	0.1180	0.1144	0.1092
Σ _S , cm. ⁻¹	2.570	2.499	2.640	2.606	2.694
$\bar{\xi}$	0.9450	0.9275	0.9455	0.9400	0.9545
D, cm.	0.3298	0.3378	0.3300	0.3345	0.3110
Σ _{aR} th , cm. ⁻¹	0.001,782	0.002,458	0.000,047	0.000,050	0.000,040
τ, cm. ²	32.85	34.70	31.60	32.50	29.90

Table 5. (Continued)

	LOPO	HYPO	RRR	SUPO	NAA-WBNS
$\pi_1 = \frac{B^2 D}{\Sigma a_R^{th}}$	7.195	5.330	281.0	258.6	307.1
$\pi_2 = \epsilon$	1.00	1.00	1.00	1.00	1.00
$\pi_3 = \nu$	2.43	2.43	2.43	2.43	2.43
$\pi_4 = \bar{\xi}_5$	0.9450	0.9275	0.9455	0.9400	0.9545
$\pi_5 = \Sigma_F^2 \tau$	0.0975	0.2072	0.2102	0.1902	0.1638
$\pi_6 = \frac{\Sigma_F}{\Sigma_a}$	0.6345	0.6575	0.6915	0.6685	0.6760
$\pi_7 = \frac{\Sigma a_R^{th}}{\Sigma_a}$	0.020,700	0.020,900	0.000,396	0.000,439	0.000,363
$\pi_8 = \frac{\Sigma a_R^{th}}{\Sigma_B}$	0.000,693	0.000,984	0.000,018	0.000,019	0.000,015
$\pi_9 = \frac{D}{\tau \Sigma_a}$	0.1166	0.0827	0.0885	0.0899	0.0952

VI. DESIGN CURVES

Curves based on the data listed in Table 5 are presented and described in this section. Curves are not presented to show the dependence of π_1 on π_2 and π_3 since these π_1 terms have been shown to be constant for the purposes of this investigation.

Figure 1 indicates the dependence of neutron age on the atom fraction of hydrogen present in the system. This variation is to be expected from the definition of neutron age and tends to substantiate the method of age calculation.

Figure 2 shows that a nearly constant value of π_4 is apparent over the entire range of π_1 values indicating that $\bar{\xi}$ is relatively insensitive to the system changes considered in this investigation. A curve joining the five points was not drawn due to the large difference in connotation which could result. A vertical line would imply that π_4 is a constant whereas a slight slope would imply that large changes in π_1 occur with slight adjustments in π_4 .

Figures 3 and 7 failed to show sufficient convergence to permit a curve to be drawn connecting the points. It is interesting to note that in both of these figures, the abscissas, π_5 and π_9 , are primarily dependent upon the critical mass. This would seem to indicate the possibility of another variable being required for the complete description of the system.

Figure 4 indicates the small variation experienced in π_6 . The slope could be accounted for by the increased absorption due to hydrogen, relative to the total absorption, which was indicated by the calculations for the low enrichment reactors.

Figure 5 indicates a definite trend in the variation of π_1 with π_7 , both of which contain the enrichment dependent term, Σ_{aR}^{th} . By comparing π_1 with π_7 , it is apparent that as Σ_{aR}^{th} decreases without bound (higher enrichments) the value of π_1 would approach infinity as π_7 approaches zero. For increasing values of Σ_{aR}^{th} (lower enrichments) the reverse would be true. This is substantiated by the figure. In practice these extremes could not be attained since the use of 100% and 0% U^{235} concentrations would be implied. These concentrations are beyond current technology.

Figure 6 indicates a relatively smooth variation of $\frac{1}{\pi_1}$ with π_8 . When π_1 was plotted as a function of π_8 , a curve similar to Figure 5 was obtained. By using $\frac{1}{\pi_1}$ as the ordinate, the uncertainty in the curvature of the figure between the high and the low points was largely eliminated. Figure 6 would be expected to pass through the origin of the curve since the expression for both coordinates contains Σ_{aR}^{th} in the numerator. The upper curve in Figure 6 was plotted by using the theoretical value of B^2 in the calculation of π_1 . The theoretical value of B^2 was obtained by solving Equation (12) for B^2 and substituting the values for the remaining variables.

In order to solve the equation, the assumption was made that [3, p. 216]

$$e^{-B^2\tau} \approx \frac{1}{1 + B^2\tau} \quad (40)$$

This assumption is valid for large reactors, i.e., k_{eff} approximately equal to unity. The expression for B^2 as obtained from Equations (12) and (40) is

$$B^2 = \frac{\epsilon v \frac{\Sigma_f}{\Sigma_a} \exp \left[-\frac{C_3}{\tau} \left(\frac{\Sigma_{aR}^{th}}{\Sigma_s} \right) C_4 \right] - 1}{\frac{D}{\Sigma_a} + \tau} \quad (41)$$

The variation between the observed and theoretical curves in Figure 6 could be due to the fact that the five reactors considered were reflected while Equation (12) applies strictly to unreflected reactors.

As previously indicated, Figure 7 failed to show definite correlation between π_1 and π_9 .

Figure 8 shows the correlation between π_5 and π_9 , the abscissas of Figures 3 and 7. This figure could be used to replace either Figure 3 or Figure 7 in a complete set of design curves.

The curves which are presented in Figures 4, 5, 6 and 8 are only suggestions as to how complete data might appear. They are based only on data from the aqueous homogeneous water boiler type reactor fueled with uranium enriched in the U^{235} isotope. It is possible that the shape of the curves could change considerably if reactors of the liquid metal or molten salt type were considered.

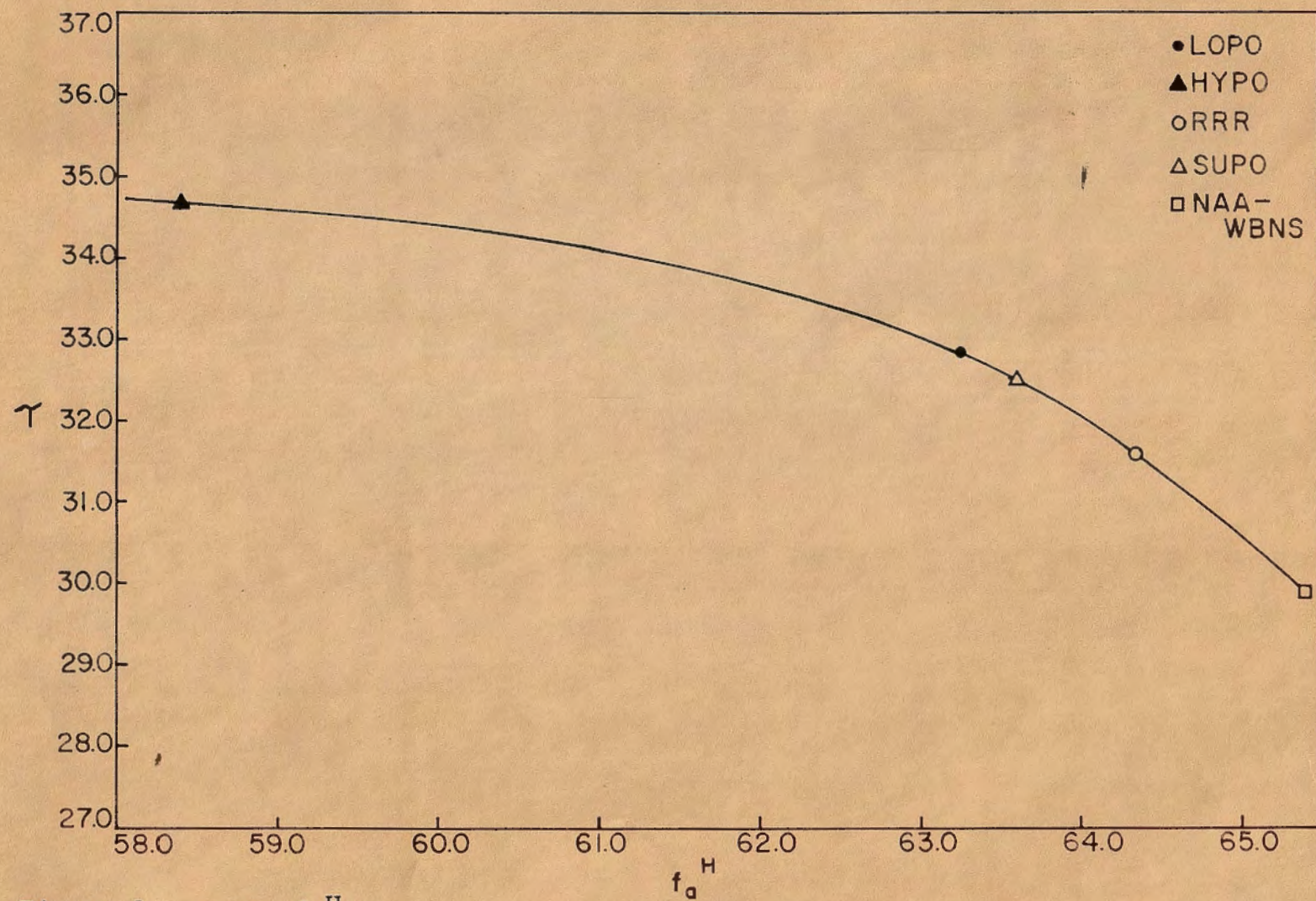


Figure 1. τ vs. f_a^H

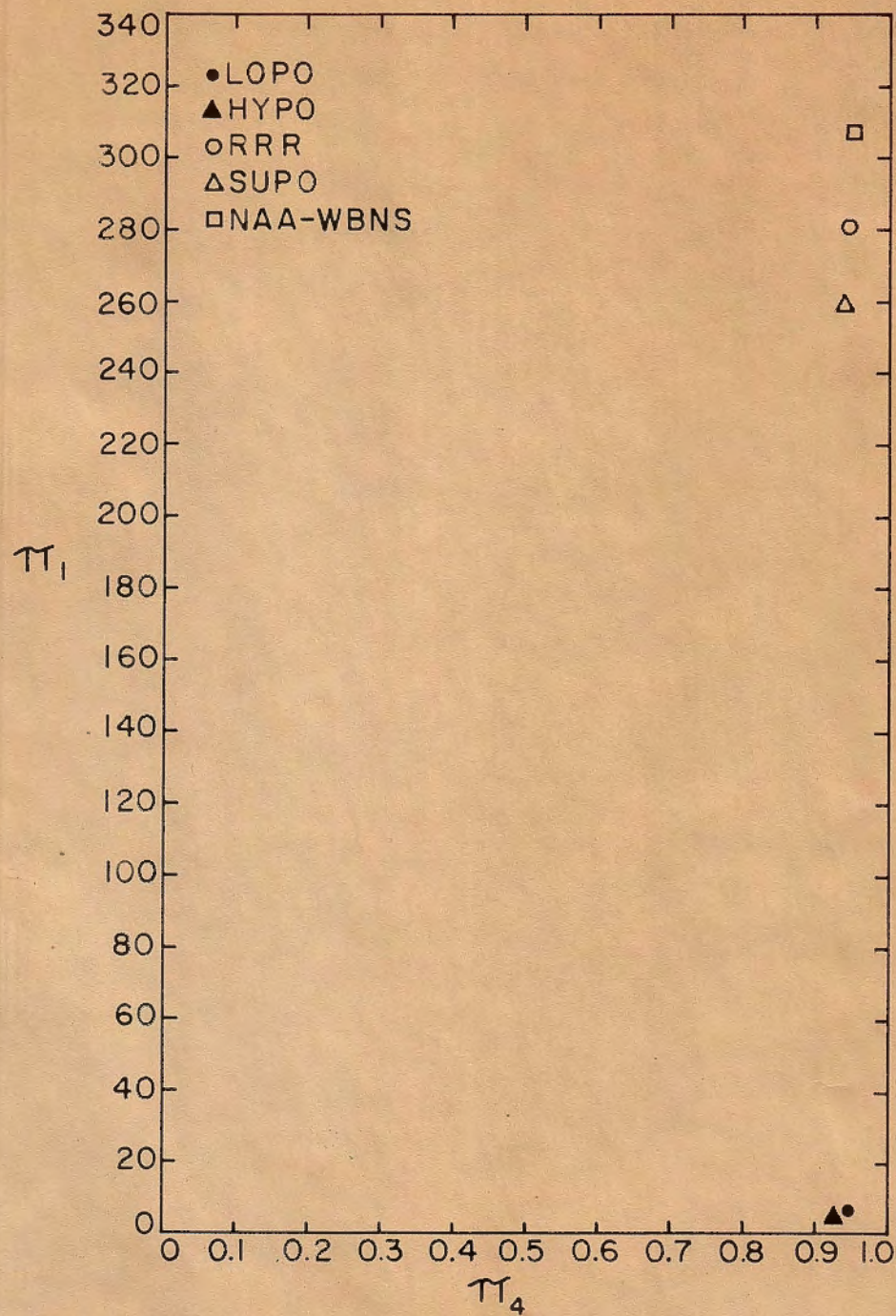


Figure 2. π_1 vs. π_4

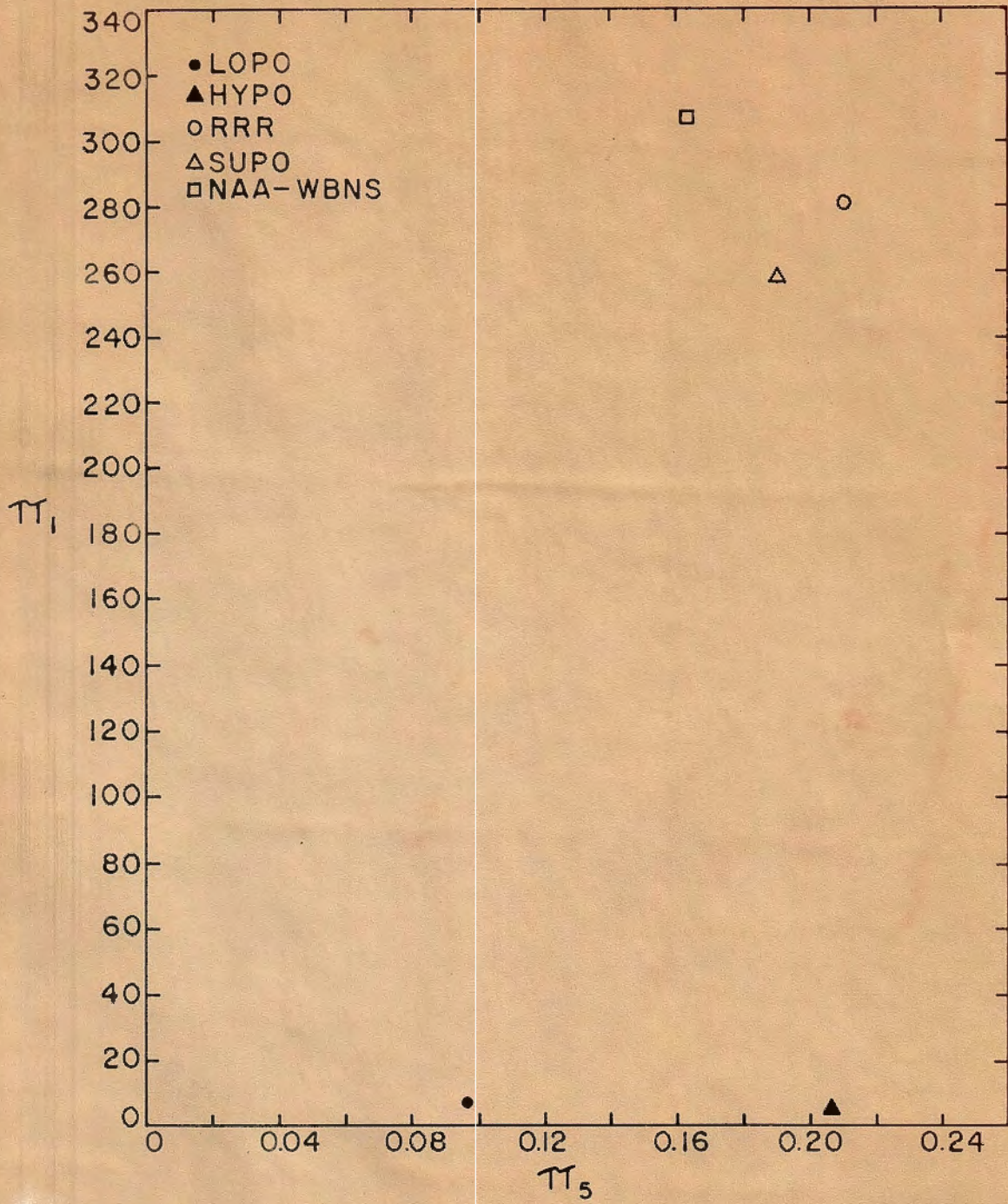


Figure 3. π_1 vs. π_5

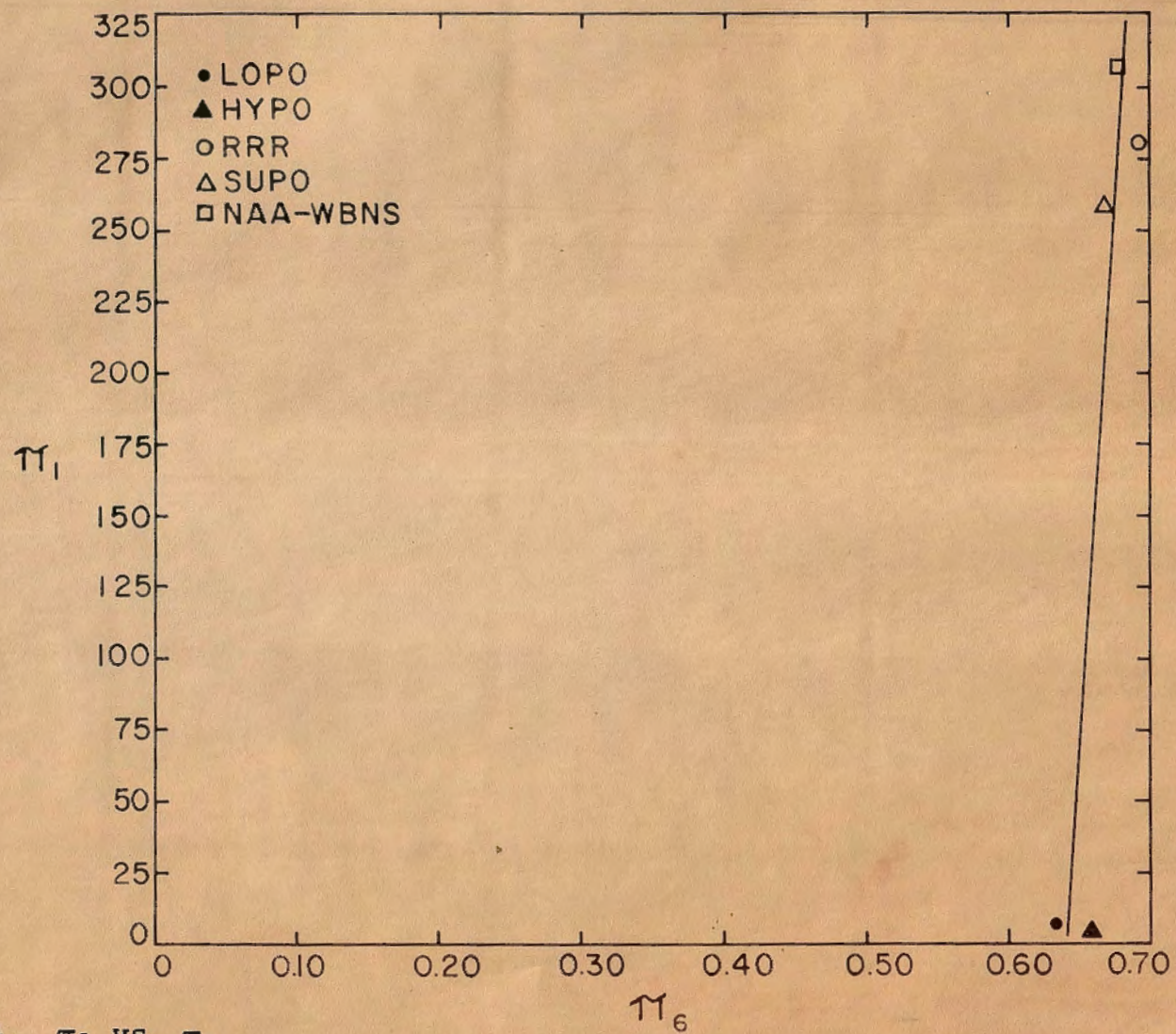


Figure 4. π_1 vs. π_6

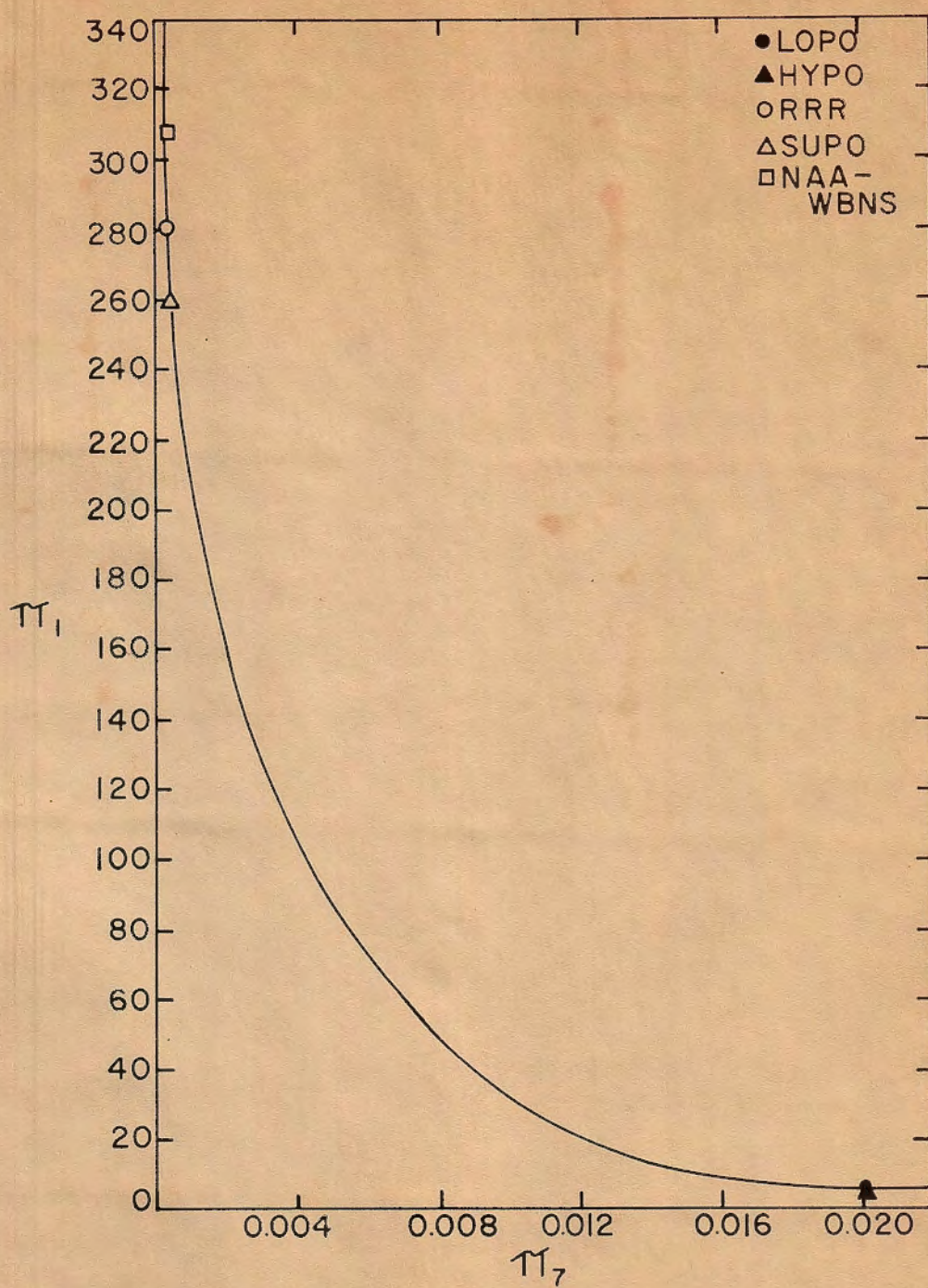


Figure 5. π_1 vs. π_7

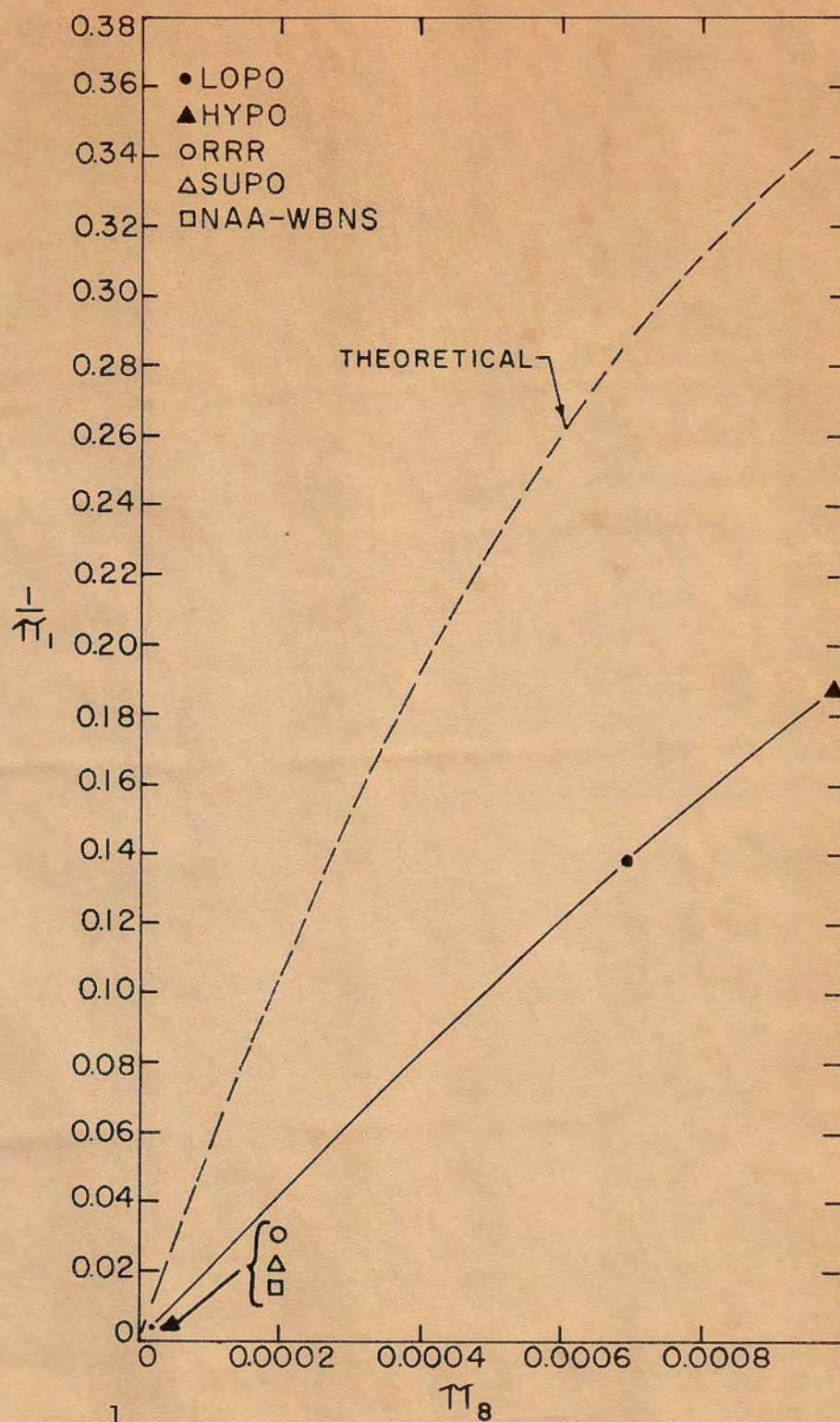


Figure 6. $\frac{1}{\pi_1}$ vs. π_8

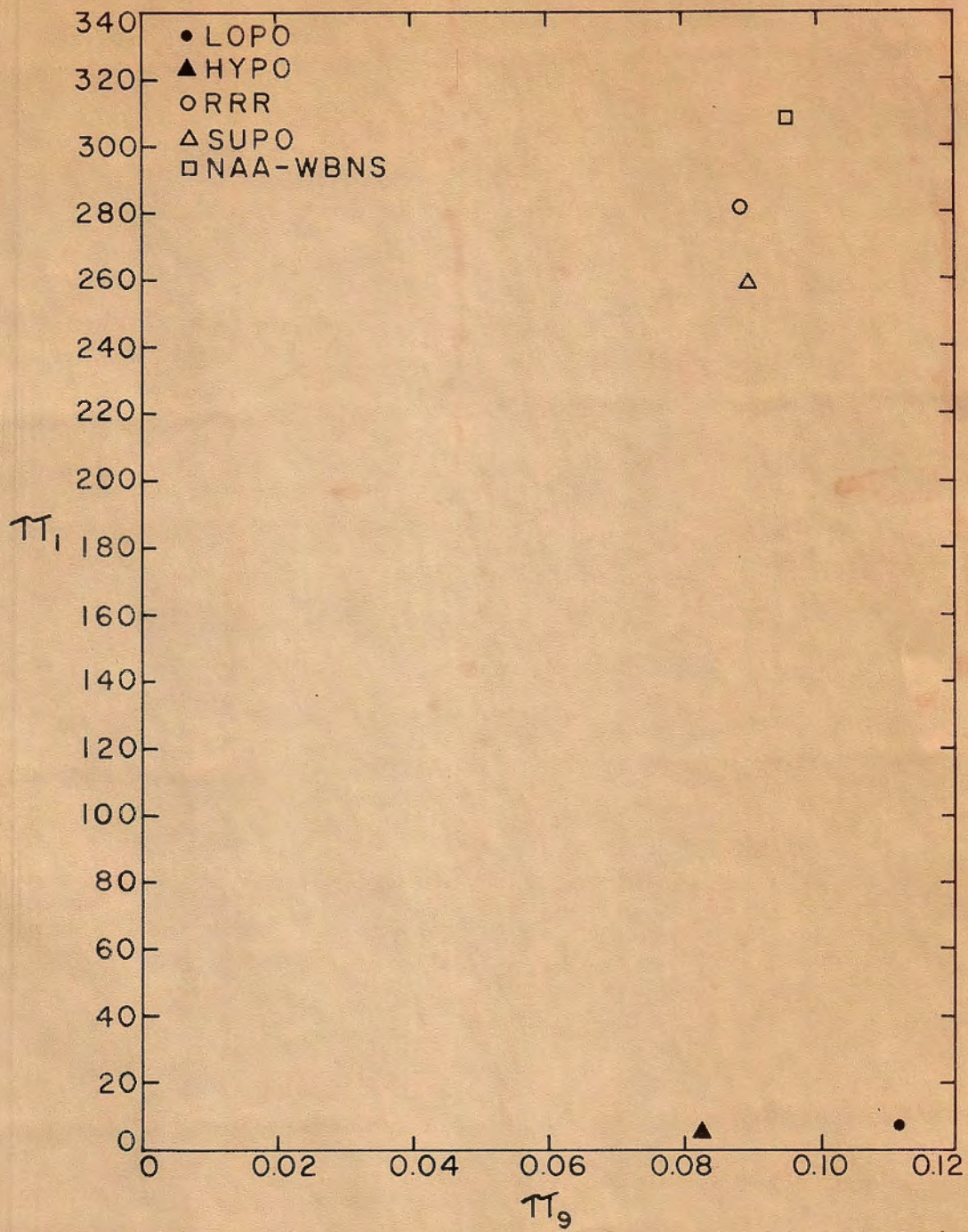


Figure 7. π_1 vs. π_9

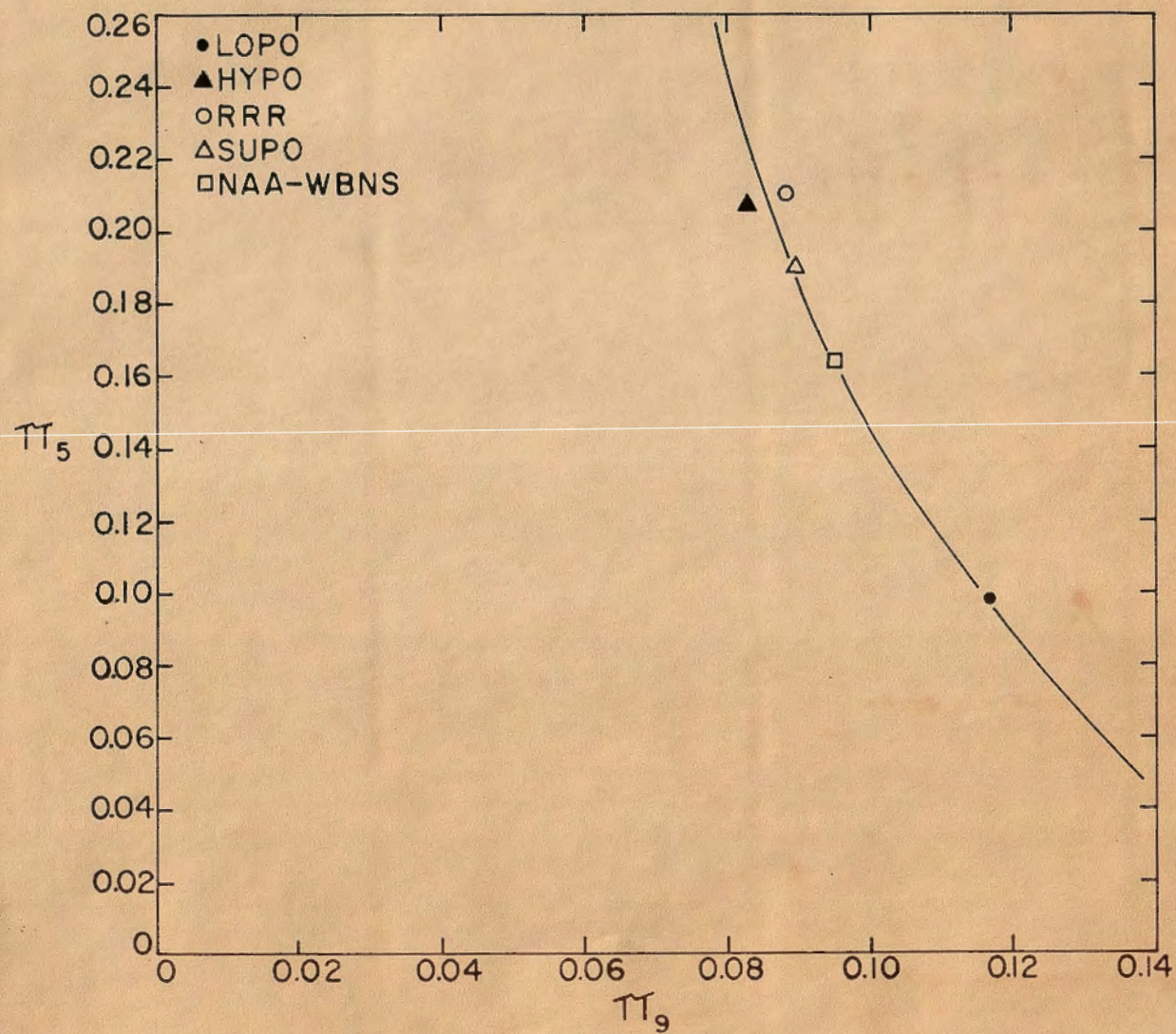


Figure 8. π_5 vs. π_9

VII. SUMMARY AND CONCLUSIONS

In this investigation, dimensional analysis considerations have been applied to the variables which describe the properties of a critical nuclear reactor. The variables chosen for the investigation corresponded with those which are used in the age-diffusion theory representation of a critical reactor considering modified one-group neutron theory. A series of dimensionless π terms were proposed and were applied to data taken from five operational reactors. Curves were then plotted to indicate the relationships between the various π terms. An attempt was then made to explain these relationships in terms of the inherent differences in the reactors.

Although it is realized that five experimental points are not sufficient to permit definite conclusions to be drawn, it is felt that there is sufficient evidence to indicate definite trends. Except in the cases of π_5 and π_9 , it is felt that definite relationships between π_1 and the various π terms are indicated. It is also realized that the five reactors considered as examples for this investigation constituted a specific reactor type. However, it is felt that the method could be applied to any critical homogeneous or quasi-homogeneous system with comparable results.

The scatter of the points indicated in the figures, particularly Figures 3 and 7, can possibly be explained by the

multidependence of π_1 on the remaining variables. For example, in Figure 3 values of π_1 are plotted against π_5 , but π_7 and π_8 , which are major variables, are not constant and their influence may distort the apparent relationship between π_1 and π_5 . Similarly, in Figure 7 the influence of π_5 and π_8 may distort the apparent relationship between π_1 and π_9 .

The various methods which have been developed to date for estimating the conditions in a critical reactor give results which compare well with experimental data. However, if the method of generating design curves through the application of dimensional analysis as indicated in this investigation was to be developed to a comparable degree, it is felt that much of the tedious computation time required for the present methods could be eliminated. By compiling sets of design curves, various fuels, moderators, reactor sizes and shapes, fuel rod designs and power levels could be evaluated by determining the changes to be expected in the dimensionless groups. For example, if it was desired to design a reactor having a certain composition and enrichment, the values of Σ_{ar}^{th} and Σ_a could be calculated to obtain π_7 . A value of π_1 could then be obtained from the curves. A value for D could be obtained from the solution composition to permit the buckling to be obtained from π_1 . The size and shape of the proposed reactor could then be determined. By so doing, calculation of several of the parameters required for a complete solution of the critical equation is not required.

VIII. SUGGESTIONS FOR FUTURE INVESTIGATIONS

After this method of generating design curves through the application of dimensional analysis has been substantiated by more complete experimental data from operational reactors, it should lend itself well to the field of nuclear engineering. The method probably could be made more accurate by incorporating multigroup neutron theory. By so doing, several new variables would be added and it is doubtful if more than one new dimension (weight) would be added. It is conceivable that the number of π terms required would soon become unwieldy causing the method to defeat its purpose--ease of making first approximations. The list of π terms listed in Table 4 could possibly be replaced by a list containing more meaningful terms; for example, $B^2\tau$ which is a measure of fast leakage as indicated by Equation (3) and $\frac{B^2D}{\Sigma_a}$ which is a measure of thermal leakage as indicated by Equations (4) and (11). Also, the dimensionless variables ϵ , v and ξ might be incorporated into a π term which would represent the multiplication.

A very important application of the method can be found in the field of power reactors. It is felt that design curves could be obtained by using data concerning both the critical mass and the operating mass of fissionable fuel in conjunction with excess reactivity information. In an application of this type, it is probable that the effect of control rods would complicate the method considerably.

The application of the method to heterogeneous reactors should be possible by applying the theory of heterogeneous reactors as found in many nuclear physics texts. This application would also add to the variables without increasing the number of dimensions by more than one.

By properly applying the techniques of dimensional analysis to the problems of nuclear engineering, it is possible that the method could prove useful to the same extent that it has in the fields of heat transfer and fluid flow.

IX. LITERATURE CITED

1. Pearlstein, S. Reactor Similitude. Nuclear Science and Engineering. 5: 269-270. April 1959.
2. MacAlpine, John Campbell, III. Design of Nuclear Reactor Models. Unpublished M.S. Thesis. Ames, Iowa, Library, Iowa State University of Science and Technology. 1960.
3. Glasstone, Samuel and Edlund, Milton C. The Elements of Nuclear Reactor Theory. Princeton, N. J., D. Van Nostrand Company, Inc. 1952.
4. Murray, Raymond L. Introduction to Nuclear Engineering. Englewood Cliffs, N.J., Prentice-Hall, Inc. 1954.
5. Glasstone, Samuel. Principles of Nuclear Reactor Engineering. Princeton, N. J., D. Van Nostrand Company, Inc. 1955.
6. Lane, James A., MacPherson, H. G. and Maslan, Frank. Fluid Fuel Reactors. Reading, Mass., Addison-Wesley Publishing Company, Inc. 1958.
7. Weinberg, Alvin M. and Wigner, Eugene P. The Physical Theory of Neutron Chain Reactors. Chicago, Ill., University of Chicago Press. 1958.
8. Hughes, Donald J. New "World-Average" Thermal Cross Sections. Nucleonics. 17, No. 11: 132-133. 1959.
9. Safford, George J. and Havens, William W., Jr. Fission Parameters for U^{235} . Nucleonics. 17, No. 11: 134. 1959.
10. Sullivan, William H. Trilinear Chart of Nuclides. 2nd ed. Washington, D. C., U. S. Govt. Print. Off. 1957.
11. Murray, Raymond L. Nuclear Reactor Physics. Englewood Cliffs, N. J., Prentice-Hall, Inc. 1957.
12. Davis, M. V. and Hauser, D. T. Thermal Neutron Data for the Elements. Nucleonics. 16, No. 3: 87-89. 1958.
13. Hughes, D. J. and Harvey, J. A. Neutron Cross Sections. U. S. Atomic Energy Commission Report BNL-325. [Brookhaven National Laboratory, Upton, N. Y.] 2nd ed. 1958.

14. Murphy, Glenn. Similitude in Engineering. New York, N. Y., The Ronald Press Company. 1950.
15. Charpie, R. A., Hughes, D. J., Littler, D. J. and Trocheris, M. Progress in Nuclear Energy, Series II: Reactors, Volume 1. London, England, Pergamon Press. 1956.
16. Los Alamos Scientific Laboratory. An Enriched Homogeneous Nuclear Reactor. U. S. Atomic Energy Commission Report AECD-3059 [Technical Information Service, AEC.]. January 25, 1951.
17. Beck, Clifford K. Nuclear Reactors for Research. Princeton, N. J., D. Van Nostrand Company, Inc. 1957.
18. King, L. D. P. The Los Alamos Homogeneous Reactor, SUPO Model. U. S. Atomic Energy Commission Report LA-1301 [Los Alamos Scientific Laboratory, N. Mex.]. February 7, 1952.
19. Remley, M. E. Operation of a Water Boiler Neutron Source. U. S. Atomic Energy Commission Report NAA-SR-839 [North American Aviation, Inc., Downey, Calif.]. March 15, 1954.

X. ACKNOWLEDGEMENTS

The author wishes to acknowledge his sincere gratitude to Dr. Glenn Murphy, Head of the Department of Theoretical and Applied Mechanics and the Department of Nuclear Engineering, for his original suggestion of the project and for his many helpful suggestions, continued support and extreme interest throughout the investigation.

Recognition is extended to Mr. John MacAlpine of the Ames Laboratory for discussing the related work he has done.

Appreciation is also expressed to the author's wife, Elizabeth, for her patience, aid and continued moral support during the course of the investigation.